C. R. Chimie 19 (2016) 1424–1431

Contents lists available at ScienceDirect

Comptes Rendus Chimie

www.sciencedirect.com

Full paper/Mémoire

Combination of X-ray synchrotron radiation techniques to gather information for clinicians

Solenn Reguer [a, *], Cristian Mocuta [a], Dominique Thiaudière [a], Michel Daudon [b], Dominique Bazin [c]

[a] Synchrotron SOLEIL, L'Orme des Merisiers, Saint-Aubin, BP 48, 91192 Gif-sur-Yvette, France
[b] Service d'Explorations Fonctionnelles, AP-HP, Hôpital Tenon, 4, rue de la Chine, 75020 Paris, France
[c] CNRS–LCMCP–UPMC, Collège de France, 11, place Marcellin-Berthelot, 75005 Paris, France

ARTICLE INFO

Article history:
Received 26 November 2014
Accepted 2 March 2015
Available online 20 February 2016

Keywords:
Nephrolithiasis
Arthritis
Osteoporosis
X-ray fluorescence spectroscopy
X-ray scattering
X-ray absorption spectroscopy

ABSTRACT

Among the different techniques specific to synchrotron radiation, the combination of X-ray absorption spectroscopy with X-ray scattering experiments is a powerful tool to characterize samples with a capability to gather structural and electronic information at the cellular level. In the present contribution, selected examples making use of such techniques point out as well the information that one can have access to. Via the presentation of the physicochemical data, this paper focuses on displaying the information that has a significant clinical character.

1. Introduction

The possibility to obtain complementary information such as crystalline structure, elemental composition and chemical speciation using non-destructive techniques is a necessary requirement in the research proposals applied to medical investigations as metal alloys and prostheses, elasticity and probes, and trace elements and nephrotoxicity. Indeed, the samples studied, coming from human bodies' specimens, are precious, volume limited and complex. They often present a heterogeneous distribution of chemical elements. In addition the morphology and structure of crystallites (or amorphous compounds) constituting the samples are supposed to be pathology dependent. The most important objective is to determine the local environment of specific chemical elements, and particularly metal ions in such biological compounds. This is however generally a difficult task. The measurements have to be done at the micrometer scale to determine both local order and elemental distribution in the samples studied.

The purpose of the present short review is to describe the opportunities given to the medical community by the use of X-ray synchrotron radiation techniques. The intent is not to provide a comprehensive summary of all the work described in the literature but to give to clinicians useful information by concentrating on particular studies using synchrotron radiation.

The examples presented in this paper were mostly performed at the DiffAbs beamline, implemented at SOLEIL synchrotron (France). This beamline led to numerous major scientific breakthroughs in materials sciences, thanks to the available almost simultaneous combination of the following techniques: X-Ray Diffraction (XRD), X-Ray Fluorescence (XRF) and X-ray Absorption Spectroscopies (XAS). As an aid toward a better description of the sample, the combination between XRD, XRF and XAS is of primary

* Corresponding author.
E-mail address: solenn.reguer@synchrotron-soleil.fr (S. Reguer).

http://dx.doi.org/10.1016/j.crci.2015.03.012

importance in the case of pathological calcifications in which it is thus possible to assess the environment of trace elements and get a precise structural description of the calcification. In addition, the possible access to a local probe (about a few μm) allows us to determine the distribution of the characterized compounds on the studied materials.

After a brief description of the DiffAbs beamline, recent results obtained on different kinds of biological entities including pathological calcifications will be presented [1,2]. Of note, the very first set of data collected on the SOLEIL Synchrotron was on the DiffAbs beamline and from kidney stone samples [3,4].

2. DiffAbs beamline

At SOLEIL Synchrotron, the DiffAbs beamline is located on a bending magnet. A permanent magnetic field of 1.71 T yields a critical energy of 8.6 keV and the horizontal angular aperture is 6 mrad. The beamline provides a monochromatic X-ray beam, tunable in the 3–23 keV energy range and can presently operate in two modes detailed hereafter: the standard beam mode obtained with the main optics and the microbeam mode by adding a secondary focusing optics.

The main optical system includes a monochromator located between two long mirrors (50 nm Rh-coated Si). The use of these two mirrors that collimate and focus the beam in the vertical plane results in a high rate of harmonic rejection and an increase of the energy resolution. The fixed-exit double crystal monochromator is composed of two independent Si(111) crystals. The first crystal, that is flat, allows the monochromatisation of the incident beam by setting the incident angle and thus selecting only the X-ray energy for which the Bragg law is fulfilled. The second crystal, that is mechanically bendable, restores the parallelism between the incoming and outgoing beam and provides a sagittal focusing (in the horizontal plane) of the monochromatic beam. This main optical set-up allows us to obtain a monochromatic beam size less than $300 \times 300\ \mu m^2$ (H × V, Full Width Half Maximum) at the sample position, with a photon flux of about 10^{12}–10^{13} ph s^{-1}.

The secondary optical system consists of two trapezoidal shaped orthogonally placed curved mirrors (Rh coated) under grazing incidence (in the Kirkpatrick Baez geometry): each of them is focusing the X-ray beam in one direction. The beam size obtained at the sample position is about $5 \times 5\ \mu m^2$ (H × V, FWHM) with a flux close to 10^{10} ph s^{-1}. Apart from the obtained small and intense X-ray spot, one of the great advantages of using KB focusing optics is their achromaticity, making them the optics of choice for laterally resolved spectroscopic experiments, in particular EXAFS (Extended X-Ray Absorption Fine Structure) measurements. The applications presented in the present paper and performed at DiffAbs were mainly realized using the microbeam set-up.

The main experimental instrument on the DiffAbs is a 6 + 2 circle diffractometer (Fig. 1). This high mechanical precision instrument offers an exceptional potential for all experiments on the beamline. The diffractometer consists of a goniometric system with 4 circles in the Kappa geometry for the sample orientation and a goniometric system with 2 circles, concentric with the first one, for detector positioning in the vertical and horizontal planes. This geometry corrects and improves the mechanical performance and leaves a large free volume for heavy and bulky sample environments. In addition, a motorized table for the sample position in the X-ray beam and a microscope allow us to adjust the sample on the diffractometer and perform X-ray imaging.

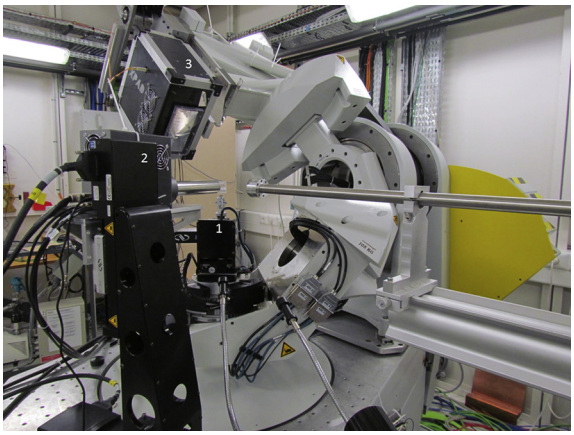

Fig. 1. The 6 + 2 circles diffractometer in Kappa Geometry on the DiffAbs beamline with (1) sample positioning using micrometric motorized tables, (2) SDD-4E detector for XRF measurements, (3) hybrid pixel area detector XPAD for XRD measurements.

Making use of the elastic scattering and the absorption processes, several synchrotron analysis techniques based on XRD or XAS and XRF spectroscopies are available on the beamline (Wide Angle X-ray Scattering, Reflectivity, Anomalous Scattering, Diffraction Anomalous Fine Structure…). All the measurements are performed on the diffractometer using different and well-adapted detectors. Moreover, all these techniques can be used in the whole 3–23 keV energy range for both standard and micro-beam modes and with various sample environments. This originality makes it the beamline of choice to study a large variety of materials as illustrated by many different topics [5–7]. In addition the coupling of XRD, XAS and XRF spectroscopies is available to correlate the information under the same experimental conditions. It means the same X-ray spot position on the sample and thus the possibility to analyze the same area of the sample under the same physico-chemical conditions.

From XAS measurements, it is possible to determine the local order, that is the environment of the probed atoms (geometry, distance of neighbors, and speciation). By XRD, long range order is accessible, allowing, for example, the determination of the crystallized phases, the orientation, and other characteristics of crystals. The combination with the microbeam scale and XRF measurements allows a good description of the structure and distribution of the different compounds constituting the samples studied.

Thanks to these characteristics, the DiffAbs beamline is thus well adapted for a great part of biological samples, though no direct access to sub-cell lateral resolution, but it gives a lateral resolution good enough for a lot of studies.

Thus, it is possible to analyse a very small amount of material, which is interesting when sampling is limited. In addition the concentration of the chemical element measured can be very low, about a few hundred parts per million (ppm).

3. Shedding light on arthritis

As underlined by Breedveld [8], osteoarthritis, the most known form of arthritis, is common in the elderly but also affects younger people. In France during the early 1990s, 6 million new cases were reported each year [9,10] in line with the fact that worldwide 25% of adults aged over 65 years suffer from pain and disability associated with this disease. Its prevalence is expected to increase with the concomitant prevalence of obesity and aging [11]. Osteoarthritis is regarded as a complex disease whose cause is not completely understood and leads ultimately to chronic pain, restriction of joint mobility, and disability. Characterized by articular cartilage, significant modifications are also observed in other joint components including bone, menisci, synovia, ligaments, capsule, and muscles [12].

Through a panel of physicochemical techniques, among others, XAS and XRD performed on DiffAbs and using the microbeam set-up, the calcification process which involves several mechanisms was studied [13–17]. Samples correspond to the knee joint specimen obtained during arthroplasty (Fig. 2).

The samples were first analyzed through XAS at the Ca K-edge. The XANES (X-ray Absorption Near Edge Structure) spectra of these samples are compared to references in Fig. 3. A pre-peak (labeled A) is attributed to the 1s to 3d transition and the O-2p molecular orbital, an intense resonance corresponding to the 1s to 4p transition, and named the white line, is observed (labeled C). This structure includes a shoulder-like feature (labeled B) corresponding to the 1s to 4s transition. These XANES data support the fact that Ca^{2+} compounds differ between calcified and non-calcified cartilage areas. In calcified areas they appear to be mainly involved in calcifications. The fact that Ca^{2+} cations are involved in the crucial cellular process, and that cartilages are not vascularized, leads to the fact that the number of free Ca^{2+} is drastically decreased locally when calcifications are present in the articulation.

In addition, the samples were analyzed by the combination of XRF, XRD and XAS at the Zn K-edge (Fig. 4). The aim was to evaluate the possible Zn accumulation close to pathological calcifications. These measurements allowed us to correlate the distribution (especially of Ca and Zn, Fig. 4a) obtained by the XRF map with the structure of the compounds present determined by XRD (pyrophosphate, Fig. 4b) and XAS realized on some points of interest (Fig. 4c). Different Zn^{2+} species are present in calcified cartilage. It seems that part of Zn^{2+} is trapped in or at the surface of the calcification made of pyrophosphate. Thus,

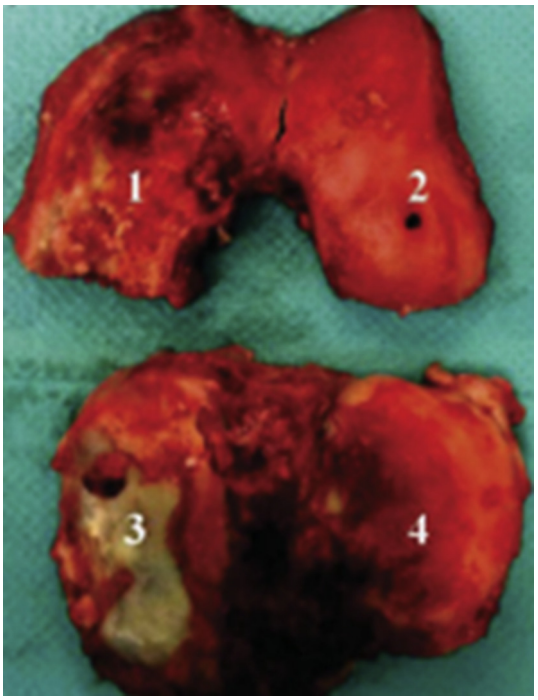

Fig. 2. Knee joint specimen obtained during arthroplasty. The specimen included femoral condyle and tibial plateau cartilage from both the medial and the lateral compartments. Cartilage areas were labeled as follows: (1) medial condyle; (2) lateral condyle; (3) medial tibial plateau; (4) lateral tibial plateau.

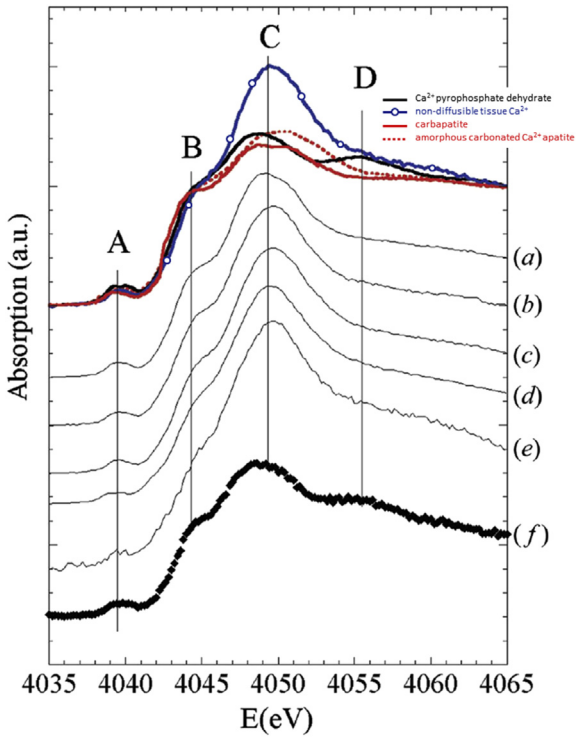

Fig. 3. XANES spectra at the Ca K-edge obtained on human osteoarthritic articular cartilage compounds and compared to carbapatite (red solid line), amorphous carbonated Ca^{2+} apatite (red dotted line), Ca^{2+} pyrophosphate dehydrate (black solid line) and non-diffusible tissue Ca^{2+} (blue solid line with circles). The (a) to (f) spectra correspond to measures on samples from patients. On theses XANES spectra, the A to D positions correspond to specific features explained in the text.

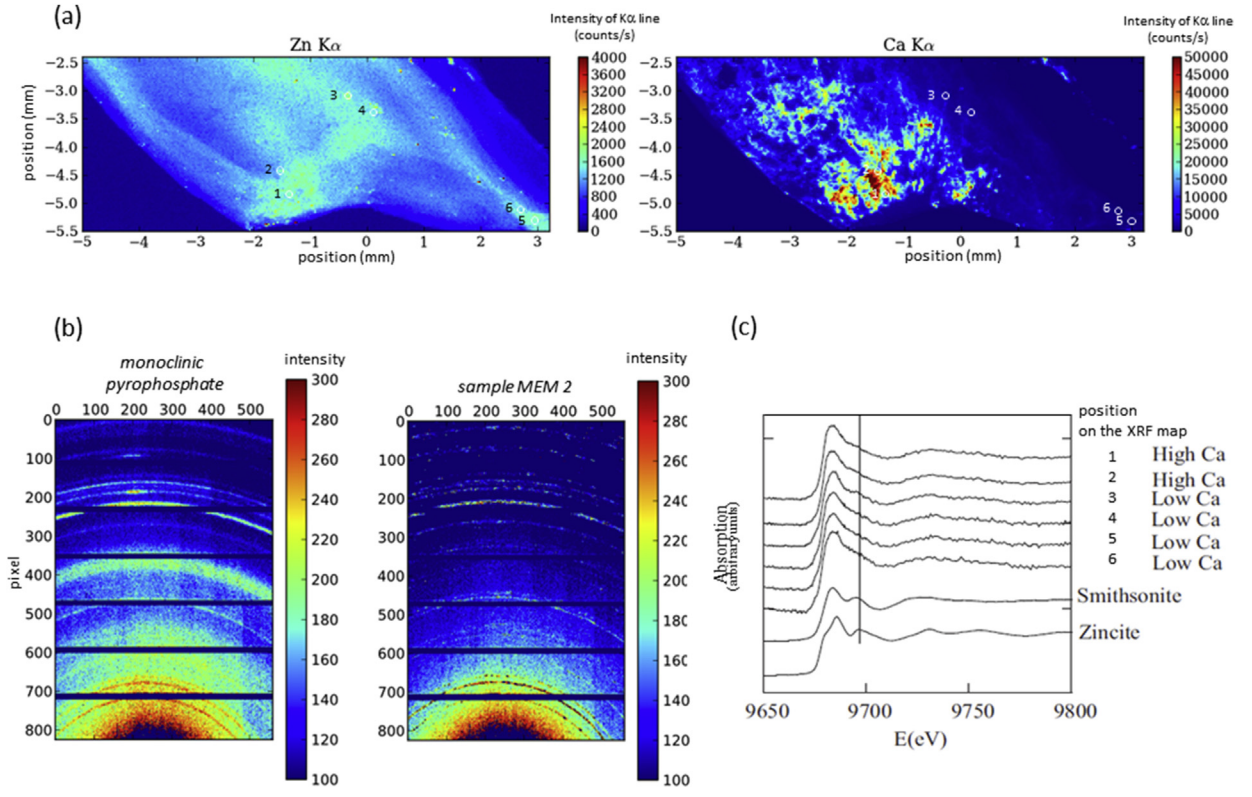

Fig. 4. (a) μXRF maps showing Zn and Ca distribution in human cartilage (sample MEM2) with points of interest (b) μXRD image using the XPAD3.2 detector on the sample MEM2 compared to a reference compound (monoclinic pyrophosphate) (c) XANES spectra obtained on the points of interest (from 1 to 6, also noted on the maps) for the sample MEM2.

calcifications present in osteoarthritis cartilage may alter the associated biological function of Zn^{2+} metalloproteins.

4. Nephrolithiasis described by XANES investigations

The relationship between vitamin D, Randall's plaque and nephrolithiasis is nowadays still debated [18]. Indeed, Randall's plaque, which serves as a nucleus of kidney stones, constitutes a major public health problem since a dramatic increase in the prevalence of kidney stones developed from a Randall's plaque is observed in western countries [19–21]. In 2010, more than 55% of calcium oxalate (CaOx) kidney stones display a Randall's plaque at their surface in young stone formers aged 20 to 30 years instead of 16% in the 1990s [22–24].

In order to determine locally (from several 10 to 100 μm scale) the structure of phases constituting such Randall's plaque, the environment of Ca was investigated [25]. The studied papillae came from two different kidneys at Nice Hospital after nephrectomy for tumor (Fig. 5). The XAS spectra, performed at the Ca K-edge on the DiffAbs beamline and using the microbeam set-up, are presented in Fig. 6 and compared to references such as biological apatite (CA for CarbApatite) and its precursor (ACCP for Amorphous Carbonated Calcium Phosphate). As from the previous example, specific features describe the spectra. While feature A is quite the same in the biological apatite (CA) and its precursor (ACCP), significant variations are measured for shoulder B as well as for the double peak at the maximum of the white line (labeled C1 and C2). Such significant differences allow us to describe precisely the environment of Ca even if the sample is hydrated.

The XANES results suggest that Randall's plaque is composed mainly of ACCP and not of CA. ACCP is evidence of an oversaturation in calcium phosphate by an excess of calcium and/or phosphate and/or due to a too high pH. Its presence in increasingly young subjects raises the question: does nutrient-enriched food specially aimed at young children affect the physiology of the kidney? The debate is still open.

5. Osteoporosis and strontium ranelate, the local environment of Sr^{2+}

Osteoporosis, characterized by an increase in bone fragility due to low bone mass and deterioration of bone quality, affects an estimated 75 million people in Europe, USA and Japan corresponding to more than 8.9 million fractures annually [26]. The public health burden of osteoporotic fractures will rise in future generations, due in part to an increase in life expectancy. Recently, strontium-drug has been introduced as a pharmacological agent for the treatment and prevention of osteoporosis and has shown anti-fracture efficacy in the treatment of postmenopausal osteoporosis [27–29].

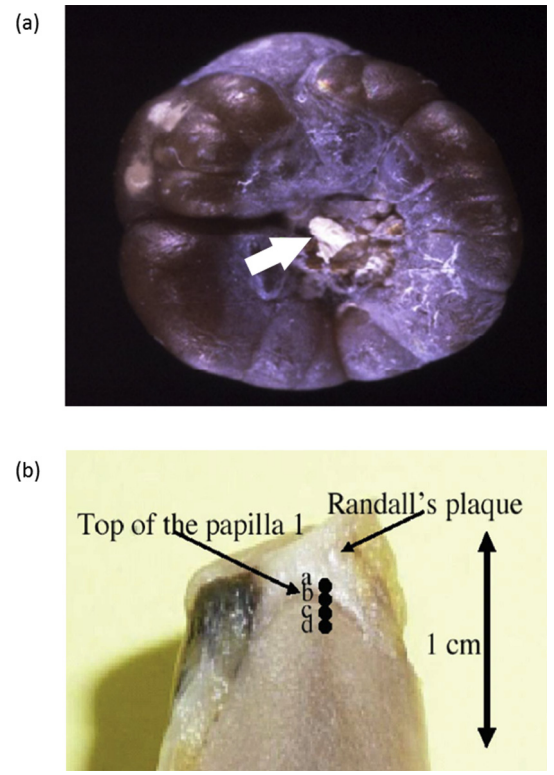

Fig. 5. studied samples: (a) Randall's plaque (white deposit) at the surface of kidney stone (b) Randall's plaque (white deposit) at the surface of a papilla.

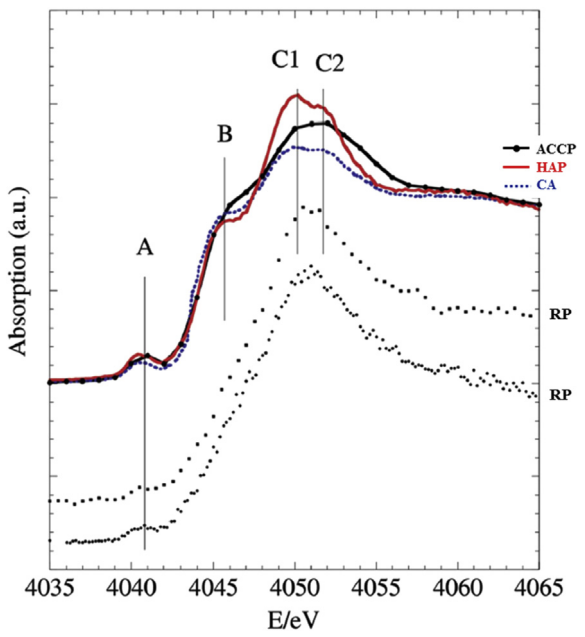

Fig. 6. XANES spectra at the Ca K-edge of two Randall's plaque (RP, dot lines) is compared to reference compounds; synthetic well crystallized stoichiometric Ca phosphate apatite (HAP, red), crystallized biological Ca phosphate apatite (CA, blue dots) exhibiting nm sized crystals, amorphous carbonated calcium phosphate (ACCP, black with circles).

Different techniques have been used to assess the localization of Sr^{2+} cations in human bones. For example, Rossi et al. [30] have collected electron energy loss near edge structures from P, C, Ca and Sr and showed physico-chemical modifications in the bone mineral at the nano-scale caused by the systemic administration of strontium ranelate. In order to observe mineralization changes, Busse et al. [31] have performed quantitative backscattered electron imaging and energy-dispersive X-ray analyses combined with micro-XRF. The complete study suggests that strontium ranelate might be considered as a therapeutic option for patients following long-term bisphosphonate treatment. The proton induced X-ray emission (PIXE) method can also be used for the determination of elemental concentrations in femoral heads [32]. More recently, Wohl et al. [33] have evaluated the accumulation of strontium in bones through in vivo XRF in rats supplemented with strontium citrate and strontium ranelate. Scattering techniques can be used but as underlined in a recent publication [34], these techniques [35–38] are sensitive to Sr content within the mineral crystals but ignore other types of non-crystalline strontium deposits.

Several academic research studies [39–43] have evaluated the modifications of the crystal size during the insertion of Sr^{2+} cations into apatite. Bigi et al. [41] and Suganthi et al. [43] found very different results regarding the effect of Sr^{2+} on the crystallinity and the crystallite size of hydroxyapatite (HAP). In fact, the complete set of such studies indicates clearly that the insertion of Sr^{2+} cations in apatite is a complex process which is very sensitive to preparation methods. Structural investigation through XAS has also been performed [44–50].

The local environment of Sr^{2+} cations in biological apatites (Fig. 7) present in pathological and physiological calcifications in patients without such Sr-based drugs was assessed through XAS experiments on DiffAbs [51,52].

The different structural hypotheses (Fig. 8a) regarding the localization of Sr^{2+} cations in bone which take into

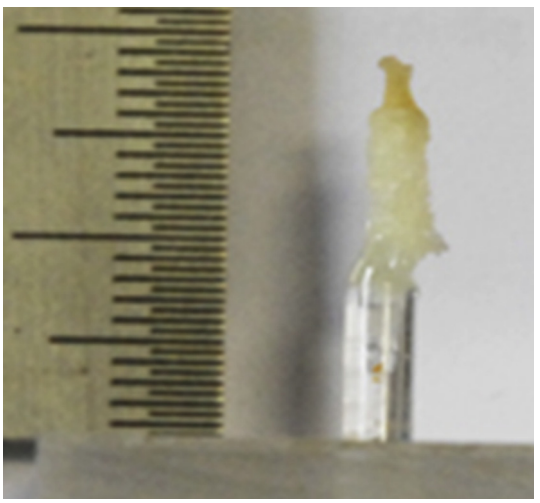

Fig. 7. Illustration of the typical physiological sample investigated in this study.

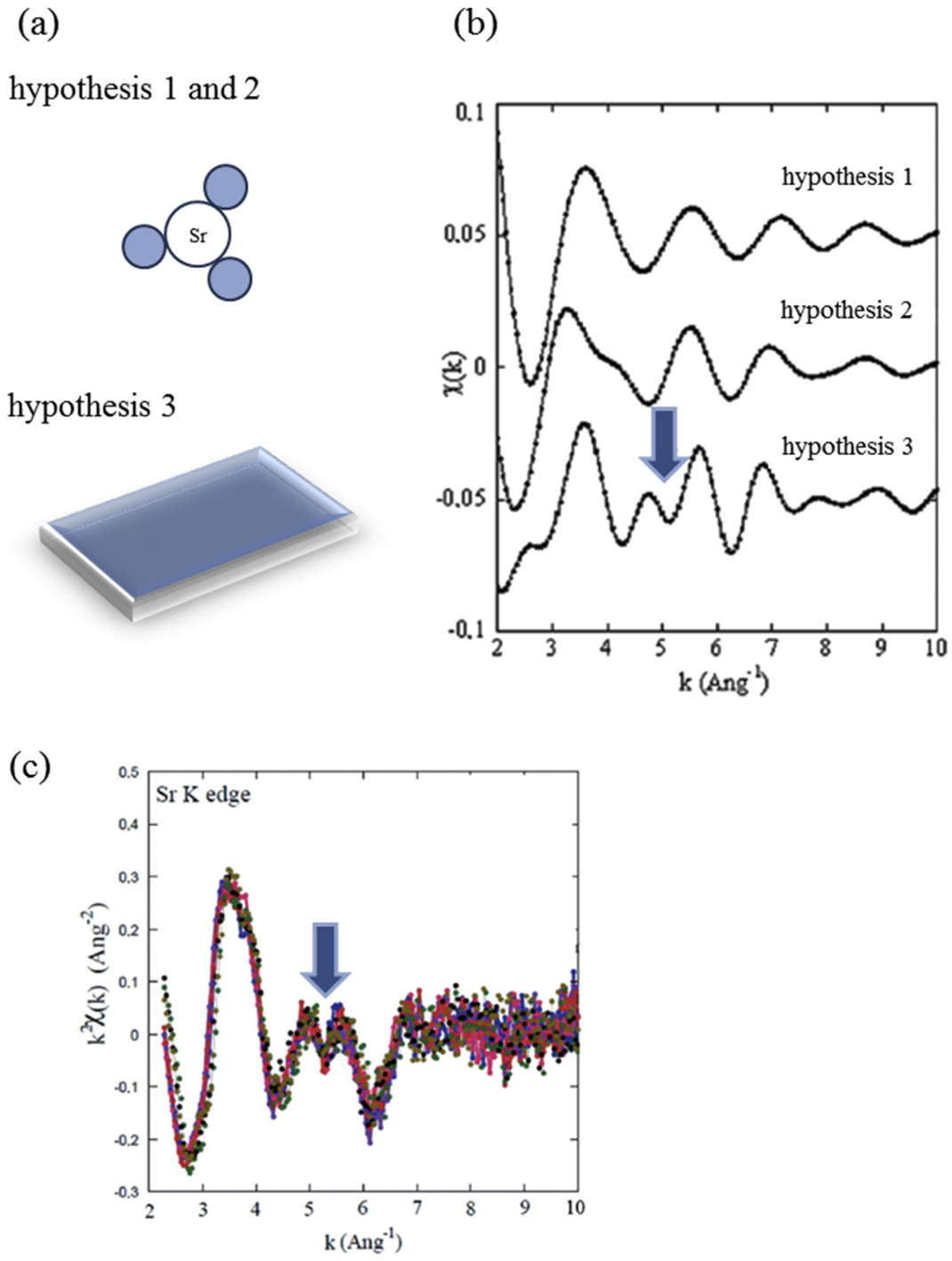

Fig. 8. (a) Three different structural hypothesis regarding the adsorption at the surface of Ca phosphate apatite of Sr^{2+} cations or its insertion. (b) EXAFS modulations of the absorption coefficient as calculated for each structural hypothesis. (c) EXAFS modulations after the Sr K-edge for different samples.

account the physicochemistry of biological apatite have been presented previously [52].

- hypothesis I : Sr^{2+} cations, only surrounded by oxygen atoms [49,50], are adsorbed at the surface of collagen or apatite.
- hypothesis II : Sr^{2+} cations are engaged in the hydrated poorly crystalline apatite region present at the surface of calcium phosphate nanocrystals.
- hypothesis III : Sr^{2+} cations are inside Ca phosphate nanocrystals on either crystallographic site (CaI) or (CaII).

In order to assess these three different hypotheses, ab initio theoretical simulation of the XANES part of the absorption spectra and quantitative analyses taking into account multiple scattering processes of the EXAFS data were combined. In fact, EXAFS analysis seems to be the more efficient way to select a structural model (Fig. 8b). Data measured after the Sr K-edge are very similar to ones previously measured [49–54] in which Sr^{2+} cations are located inside the apatite crystal. Moreover, the complete set of experimental data collected on 17 physiological and pathological calcifications seems to indicate that there is no relationship between the nature of the calcification (physiological and pathological) and the adsorption mode of Sr^{2+} cations (simple adsorption or insertion).

6. Similar investigations on other beamlines

Research at the interface between physics, chemistry and medicine has also been performed on other beamlines implemented on other synchrotron facilities. Quite recently, Bohic et al. [55] have described the possibilities offered by XRF and XAS in the biomedical field through very interesting examples of applications performed at the ESRF synchrotron-based microspectroscopy platform. We would like to hereafter assess two examples in order to show the complexity as well as the wealth of such research.

The first example is given by Pt based drugs which are widely used in oncology [56]. To assess the electronic state as well as the local environment of Pt, XAS measurements are of great help. Indeed, the analysis of the XANES edge height provides information about the relative proportions of Pt(II) and Pt(IV) complexes [57] and the EXAFS data analysis gives important results on the surrounding environment of Pt [58–62]. Among the different breakthroughs, Serimaa et al. [63] described for the first time the Pt–Pt partial radial distribution function of a biologically active Pt complex and explained the structure by using a mixture model where the major components are mono- and bi-nuclear Pt complexes. More recently, Beret et al. [60] gave evidence of a slight hydration structure around the Pt complex. A parallel, which can be established between the chemistry of Pt drugs and that of the Pt catalyst, has been already underlined [64].

Another example is given by physiological calcifications: the major part of the investigations based on XAS measurements at the Ca K-edge is related to this physiological calcification [50,54,65–69]. Peters et al. [69] indicated that the size and morphology of the bone mineral particles are independent of the nature of the bone origin and that significant differences in the overall composition of the bone samples and in the carbonate content of the mineral phase exist. Similar results were obtained by Harries et al. [70]. Major information can be gathered also through XANES performed at the Ca $L_{2,3}$-edges as these measurements are as well indicative of the local structure around Ca and can be performed on intracellular inclusions [71–74].

7. Conclusion and perspectives

This presentation of investigations regarding pathological calcifications through different examples shows the importance of X-ray techniques using synchrotron radiation to achieve meaningful and effective analysis for medical applications. The few examples in the present paper show the crucial role of specific beamlines, such as the DiffAbs beamline at SOLEIL, where it is possible to combine different techniques, such as XRF, XRD and XAS. Particularly, imaging techniques are crucial and reveal a lot of information. Indeed, thanks to the rapid acquisition obtained by coupling the very great brightness of the synchrotron source and the temporal performances of new detectors (such as hybrid pixel detectors for example) it is now possible to realize simultaneously large XRF and XRD maps to correlate elemental and structural information. Furthermore the recent development of the “flyscan” method will strongly increase the acquisition performances, as it aims to realize acquisition in a continuous mode [75]. Another important instrument evolution on the DiffAbs beamline is linked to the current development of a new 2D hybrid pixel detector covering a large angular domain. Such instruments will allow us to perform rapid XRD measurements but also will improve the possibility of diffraction-tomography and Pair Distribution Function (PDF) analyzes.

Different technical aspects of the cited synchrotron techniques are not totally exploited and other existing techniques are not yet developed in this field. For this reason, in addition to the already interesting results obtained, the scientific studies presented in this paper also open up new ideas for next scientific development in this field of research. For example, numerous major breakthroughs, and innovative applications regarding medical nanotechnology are now available [76–78], for example, nanometre-scale metallic clusters which have interesting natural bactericidal and fungicidal properties [79]. Further research in this domain is typically required to focus on theranostics, as defined by the combination of therapeutic and diagnostic agents on the very same single nanoparticle which is emerging as a very promising therapeutic paradigm. For such nanomaterials, opportunities to perform at the same time a characterization of nanometer scale clusters by XRD and of drug containing Pt by XAS will lead to major scientific breakthroughs regarding the deciphering of their interaction with tumors [79].

Acknowledgments

This work was supported by the Physics and Chemistry Institutes of CNRS (Centre National de la Recherche Scientifique) and by contracts ANR-09-BLAN-0120-02 and ANR-12-BS08-0022 (Agence Nationale de la Recherche). The authors are grateful to the SOLEIL (Source Optimisée de Lumière d'Énergie Intermédiaire du LURE, Laboratoire pour l'Utilisation du Rayonnement Electromagnétique) Synchrotron Facility for beam time allocation and would like to very much thank the support group of SOLEIL for their help during experiment.

We also very much thank the following cited doctors for providing samples and useful discussions. Dr. I. Brocheriou, Prof. P. Jungers, Prof. B. Knebelman (Necker Hospital); Prof. P. Conort, Dr. P. Dorfmüller and Dr. I. Tostivint (Lapitié Salpêtrière Hospital); Prof. D. Hannouche, Dr. E.A. Korng, Prof. F. Lioteì, Dr. Ch. Nguyen and Dr. Ch. Chappard (Lariboisière

Hospital); Dr. J.P. Haymann, Dr. E. Letavernier, Dr. J. Rodes and Prof. O. Traxer from Tenon Hospital; Dr. X. Carpentier (Nice Hospital); Prof. M. Mathonnet (Limoges Hospital); Prof. P. Meria (St Louis Hospital); Prof. J.C. Williams (Department of Anatomy and Cell Biology, Indiana University School of Medicine, Indianapolis, Indiana, U.S.A.).

References

[1] D. Bazin, M. Daudon, C. Combes, C. Rey, Chem. Rev. 112 (2012) 5092.
[2] D. Bazin, M. Daudon, J. Phys. D Appl. Phys. 45 (2012) 383001.
[3] S. Hasnain, J. Synchrotron Radiat. 14 (2007) 297.
[4] D. Bazin, X. Carpentier, O. Traxer, D. Thiaudière, A. Somogyi, S. Reguer, G. Waychunas, P. Jungers, M. Daudon, J. Synchrotron Radiat. 15 (2008) 506.
[5] J. Monnier, S. Reguer, E. Foy, D. Testemale, F. Mirambet, M. Saheb, P. Dillmann, I. Guillot, Corros. Sci. 78 (2014) 293.
[6] C. Mocuta, M.I. Richard, J. Fouet, S. Stanescu, A. Barbier, C. Guichet, O. Thomas, S. Hustache, A. Zozulya, D. Thiaudière, J. Appl. Crystallogr. 46 (6) (2013) 1842.
[7] S. Djaziri, P.O. Renault, E. Le Bourhis, P. Goudeau, D. Faurie, G. Geandier, C. Mocuta, D. Thiaudiere, J. Appl. Phys. 116 (2014) 093504.
[8] F.C. Breedveld, Rheumatology 43 (2004).
[9] E. Levy, A. Ferme, D. Perocheau, I. Bono, Rev. Rhum. Ed. Fr. 60 (1993) 63S.
[10] M. Watson, Pharm. J. 259 (1997) 296.
[11] N. Arden, M.C. Nevitt, Best Pract. Res. Clin. Rheumatol. 20 (2006) 3.
[12] D.J. Hunter, D.T. Felson, BMJ 332 (2006) 639.
[13] H.-K. Ea, C. Nguyen, D. Bazin, A. Bianchi, J. Guicheux, P. Reboul, M. Daudon, F. Lioté, Arthritis Rheum. 63 (2011) 10.
[14] C. Nguyen, H.-K. Ea, D. Bazin, M. Daudon, F. Lioté, Arthritis Rheum. 62 (2010) 2829.
[15] C. Nguyen, H.K. Ea, D. Thiaudière, S. Reguer, D. Hannouche, M. Daudon, F. Lioté, D. Bazin, J. Synchrotron Radiat. 18 (2011) 475.
[16] C. Nguyen, D. Bazin, M. Daudon, A. Chatron-Colliet, D. Hannouche, A. Bianchi, D. Côme, A. So, N. Busso, F. Lioté, H.-K. Ea, Arthritis Res. Ther. 15 (2013) R103.
[17] H.-K. Ea, V. Chobaz, C. Nguyen, S. Nasi, P. van Lent, M. Daudon, A. Dessombz, D. Bazin, G. McCarthy, B. Jolles-Haeberli, A. Ives, D. Van Linthoudt, A. So, F. Lioté, N. Busso, PLoS One 8 (2013) e57352.
[18] M. Daudon, Arch. Pédiatr. 20 (2013) 336.
[19] A. Randall, N. Engl. J. Med. 214 (1936) 234.
[20] A. Randall, Ann. Surg. 105 (1937) 1009.
[21] A.P. Evan, J. Lingeman, F.L. Coe, E. Worcester, Kidney Int. 69 (2006) 1313.
[22] M. Daudon, O. Traxer, P. Jungers, D. Bazin, Renal Stone Dis. 900 (2007) 26.
[23] X. Carpentier, D. Bazin, C. Combes, A. Mazouyes, S. Rouzière, P.A. Albouy, E. Foy, M. Daudon, J. Trace Elem. Med. Biol. 25 (2011) 160.
[24] M. Daudon, D. Bazin, J. Phys. Conf. Ser 425 (2013) 022006.
[25] X. Carpentier, D. Bazin, P. Jungers, S. Reguer, D. Thiaudière, M. Daudon, J. Synchrotron Radiat. 17 (2010) 374.
[26] O. Johnell, J.A. Kanis, Osteoporos. Int. 17 (2006) 1726.
[27] P.J. Meunier, C. Roux, E. Seeman, S. Ortolani, J.E. Badurski, T.D. Spector, J. Cannata, A. Balogh, E. Lemmel, S. Pors-Nielsen, R. Rizzoli, H.K. Genant, J. Reginster, N. Engl. J. Med. 350 (2004) 459.
[28] P.J. Marie, Curr. Opin. Pharmacol. 5 (2005) 633.
[29] B. Cortet, Curr. Osteoporos. Rep. 9 (2011) 25.
[30] A.L. Rossi, S. Moldovan, W. Querido, A. Rossi, J. Werckmann, O. Ersen, M. Farina, Micron 56 (2014) 29.
[31] B. Busse, B. Jobke, M. Hahn, M. Priemel, M. Niecke, S. Seitz, J. Zustin, J. Semler, M. Amling, Acta Biomater. 6 (2010) 4513.
[32] Y.X. Zhang, Y.S. Wang, Y.P. Zhang, G.L. Zhang, Y.Y. Huang, W. He, NIM B 260 (2007) 178.
[33] G.R. Wohl, D.R. Chettle, A. Pejović-Milić, C. Druchok, C.E. Webber, J.D. Adachi, K.A. Beattie, Bone 52 (2013) 63.
[34] C. Li, O. Paris, S. Siegel, P. Roschger, E.P. Paschalis, K. Klaushofer, P. Fratzl, J. Bone Miner. Res. 25 (2010) 968.
[35] A. Guinier, Théorie et technique de la radiocristallographie, Dunod, Paris, 1964.
[36] N.P. Camacho, S. Rinnerthaler, E.P. Paschalis, R. Mendelsohn, A.L. Boskey, P. Fratzl, Bone 25 (1999) 287.
[37] P. Fratzl, H. Gupta, O. Paris, A. Valenta, P. Roschger, K. Klaushofer, Prog. Colloid Polym. Sci. 130 (2005) 33.
[38] P. Fratzl, S. Schreiber, K. Klaushofer, Connect Tissue Res. 34 (1996) 247.
[39] A. Bigi, M. Falini, M. Gazzano, M. Roveri, Mater. Sci. Forum 278–281 (1988) 814.
[40] Z.Y. Li, W.M. Lam, C. Yang, B. Xu, G.X. Ni, S.A. Abbah, K.M.C. Cheung, K.D.K. Luk, W.W. Lu, Biomaterials 28 (2007) 1452.
[41] A. Bigi, E. Boanini, C. Capuccini, M. Gazzano, Inorg. Chim. Acta 360 (2007) 1009.
[42] M.D. O'Donnel, Y. Fredholm, A. De Rouffignac, R.G. Hill, Acta Biomater. 4 (2008) 1455.
[43] R.V. Suganthi, K. Eayaraja, M.I. Ahymah Joshy, V.S. Chandra, E.K. Girija, S.N. Kalkura, Mater. Sci. Eng. (2015) (in press).
[44] A. Balerna, M. Bionducci, F. Falqui, G. Licheri, A. Meneghini, G. Navarra, M. Bettinelli, J. Non-Cryst. Solids 232–234 (1998) 607.
[45] P. O'Day, M. Newville, P.S. Neuhoff, N. Sahai, S.A. Carroll, J. Colloid Interface Sci. 222 (2000) 184.
[46] D.M. Singer, S.B. Johnson, J.G. Catalano, F. Farges, G.E. Brown Jr., Geochim. Cosmochim. Acta 72 (2008) 5055.
[47] A.A. Finch, N. Allison, S.R. Sutton, M. Newville, Geochim. Cosmochim. Acta 67 (2003) 1197.
[48] N. Allison, A.A. Finch, M. Newville, S.R. Sutton, Geochim. Cosmochim. Acta 69 (2005) 3801.
[49] J. Terra, E. Rodrigues Dourado, J.-G. Eon, D.E. Ellis, G. Gonzalez, A. Malta Rossi, Phys. Chem. Chem. Phy. 11 (2009) 568.
[50] C.G. Frankær, A.C. Raffalt, K. Stahl, Calcif. Tissue Int. 94 (2014) 248.
[51] D. Bazin, M. Daudon, C. Chappard, J.J. Rehr, D. Thiaudière, S. Reguer, J. Synchrotron Radiat. 18 (2011) 912.
[52] D. Bazin, A. Dessombz, C. Nguyen, H.K. Ea, F. Lioté, J. Rehr, C. Chappard, S. Rouzière, D. Thiaudière, S. Reguer, M. Daudon, J. Synchrotron Radiat. 21 (2014) 136.
[53] I. Persson, M. Sandström, H. Yokoyama, M. Chaudhry, Z. Naturforsch. A 50 (1995) 21.
[54] M. Korbas, E. Rokita, W. Meyer-Klaucke, J. Ryczek, J. Biol. Inorg. Chem. 9 (2004) 67.
[55] S. Bohic, M. Cotte, M. Salomé, B. Fayard, M. Kuehbacher, P. Cloetens, G. Martinez-Criado, R. Tucoulou, J. Susini, J. Struct. Biol. 177 (2012) 248.
[56] A.V. Klein, T.W. Hambley, Chem. Rev. 109 (2009) 4911.
[57] M.D. Hall, G.J. Foran, M. Zhang, Ph.J. Beale, T.W. Hambley, J. Am. Chem. Soc. 125 (2003) 7524.
[58] D. Bouvet, A. Michalowicz, S. Crauste-Manciet, D. Brossard, K. Provost, Inorg. Chem. 45 (2006) 3393.
[59] D. Bouvet, A. Michalowicz, S. Crauste-Manciet, E. Curis, I. Nicolis, L. Olivi, G. Vlaic, D. Brossard, K. Provost, J. Synchrotron Radiat. 13 (2006) 477.
[60] E.C. Beret, K. Provost, D. Müller, E. Sánchez Marcos, J. Phys. Chem. B 113 (2009) 12343.
[61] K. Provost, D. Bouvet-Muller, S. Crauste-Manciet, J. Moscovici, L. Olivi, G. Vlaic, A. Michalowicz, Biochimie 91 (2009) 1301.
[62] K. Provost, E.C. Beret, D. Bouvet Muller, A. Michalowicz, E. Sánchez Marcos, J. Chem. Phys. 138 (2013) 084303.
[63] R. Serimaa, V. Eteläniemi, T. Laitalainen, A. Bienenstock, S. Vahvaselkä, T. Paakkari, Inorg. Chem. 36 (1997) 5574.
[64] D. Bazin, C. R. Chimie 17 (2014) 615.
[65] J.E. Harries, D.W.L. Hukins, C. Holt, S.S. Hasnain, J. Cryst. Growth 84 (1987) 563.
[66] D. Eichert, M. Salomé, M. Banu, J. Susini, C. Rey, Spectrochim. Acta B 60 (2005) 850.
[67] K. Asokan, J.C. Jan, J.W. Chiou, W.F. Pong, P.K. Tseng, I.N. Lin, J. Synchrotron Radiat. 8 (2001) 839.
[68] R.M. Miller, D.W.L. Hukins, S.S. Hasnain, P. Lagarde, Biochem. Biophys. Res. Commun. 99 (1981) 102.
[69] F. Peters, K. Schwarz, M. Epple, Thermochim. Acta 361 (2000) 131.
[70] J.E. Harries, D.W.L. Hukins, S.S. Hasnain, Calcif. Tissue Int. 43 (1988) 250.
[71] M.E. Fleet, X. Liu, Am. Mineral. 94 (2009) 1235.
[72] E. Couradeau, K. Benzerara, E. Gérard, D. Moreira, S. Bernard, G.E. Brown Jr., P. López-García, Science 336 (2012) 459.
[73] K. Benzerara, T.H. Yoon, T. Tyliszczak, B. Constantz, A.M. Spormann, G.E. Brown, Geobiology 2 (2004) 249.
[74] K. Benzerara, N. Menguy, M. Obst, J. Stolarski, M. Mazur, T. Tylisczak, G.E. Brown, A. Meibom, Ultramicroscopy 111 (2011) 1268.
[75] K. Medjoubi, N. Leclercq, F. Langlois, A. Buteau, S. Lé, S. Poirier, P. Mercère, M. Sforna, C.M. Kewish, A. Somogyi, J. Synchrotron Radiat. 20 (2) (2013) 293.
[76] S.M. Janib, A.S. Moses, J.A. MacKay, Adv. Drug Deliv. Rev. 62 (2010) 1052.
[77] J. Xie, S. Lee, X. Chen, Adv. Drug Deliv. Rev. 62 (2010) 1064.
[78] S. Harrisson, J. Nicolas, A. Maksimenko, D.T. Bui, J. Mougin, P. Couvreur, Angew. Chem. 125 (2013) 1722.
[79] L.G. Bach, R. Islam, T.-S. Vo, S.-K. Kim, K.T. Lim, J. Colloid Interface Sci. 394 (2013) 132.